



PDF hosted at the Radboud Repository of the Radboud University Nijmegen

The following full text is a publisher's version.

For additional information about this publication click this link.

<http://hdl.handle.net/2066/193384>

Please be advised that this information was generated on 2019-06-02 and may be subject to change.

SCIENTIFIC REPORTS

OPEN

Intradermal injection of low dose human regulatory T cells inhibits skin inflammation in a humanized mouse model

Sija Landman¹, Vivian L. de Oliveira¹, Piet E. J. van Erp², Esther Fasse¹, Stijn C. G. Bauland³, Irma Joosten¹ & Hans J. P. M. Koenen¹

Recent regulatory T cell (Treg) based clinical trials support their therapeutic potential in transplantation and auto-inflammatory diseases. However, large numbers of Treg are needed to accomplish therapeutic efficacy. Local injection at the site of inflammation (targeted delivery) may lower the numbers needed for therapy. We evaluated if local delivery of low numbers of human Treg by intradermal injection was able to prevent skin inflammation, using the humanized mouse huPBL-SCID-huSkin allograft model. A dose of only 1×10^5 freshly isolated, non expanded Treg injected intradermally in close proximity to the transplanted human skin prevented inflammation of the grafted tissue induced by 4×10^7 IP injected human allogeneic PBMCs, (ratio Treg:PBMC = 1:400), as indicated by the inhibition of epidermal thickening, sustained Keratin-10 expression, the absence of Keratin-16 up regulation and prevention of human CD3+ T cell influx. A concomitant reduction of human T cells was observed in lymph nodes and spleen of the mice. Injection of Treg at the contralateral side was also shown to inhibit skin inflammation, suggesting that the inflammatory response was regulated both locally and systemically. In conclusion, local application of Treg may be an attractive way to suppress inflammation *in vivo* without the need for prior *ex vivo* expansion.

Regulatory T cells (Treg) are important in maintaining immune homeostasis¹. Due to their potential as immune modulators, Treg are studied widely for therapeutic use in order to control unwanted immune responses and to promote tolerance in transplantation, autoimmunity, and chronic inflammatory diseases^{2–5}.

Recently, a promising effect of Treg therapy with expanded FOXP3+ Treg in the prevention of graft-versus-host-disease, a common complication after allogeneic stem cell transplantation, was demonstrated^{6,7}. Currently, Treg therapy is also tested in solid organ transplantation. In living donor liver transplantation, a pilot study with *ex vivo* expanded Treg was shown to be effective and to induce operational tolerance⁸. The ONE study investigates the use of expanded Treg after living donor kidney transplantation (clinicaltrials.gov NCT02085629). These phase I/II clinical trials aim to find the optimal dose and dosing regimen as well as to characterize the best Treg subtype and *ex vivo* expansion protocol. All these studies make use of *ex vivo* Treg expansion protocols, and struggle to consistently obtain sufficient cell numbers. Also in autoimmunity and chronic inflammatory diseases, the first trials are underway. Promising results were obtained in small scale phase I/II clinical trials in type 1 diabetes (T1DM)^{9,10}, Crohn's disease¹¹ and uveitis¹². Treg function in these diseases is often hampered and optimal isolation, expansion, and injection protocols are under study¹³. As to our knowledge, no clinical studies so far have been performed in skin inflammatory diseases, like psoriasis, while also here Treg therapy may hold promise¹⁴.

Currently, in clinical trials, typically around $1–10 \times 10^6$ Treg/kg are infused systemically². This amount of cells cannot be obtained by simple blood collection and therefore Treg have to be expanded. Different *ex vivo* expansion protocols are being studied^{15–18}, however, expansion has its disadvantages. Expansion is time consuming and limits the possibilities for use in acute cases. Furthermore, due to their plasticity, Treg can convert into potentially

¹Radboud university medical center, department of Laboratory Medicine-Medical Immunology, Nijmegen, The Netherlands. ²Radboud university medical center, department of Dermatology, Nijmegen, The Netherlands.

³Bauland kliniek, Mill, The Netherlands. Correspondence and requests for materials should be addressed to H.J.P.M.K. (email: Hans.Koenen@radboudumc.nl)

inflammatory IL-17 producing cells, which is more likely to occur when cells are expanded¹⁹. When cells are given systemically/ IV, the majority of cells is lost or does not reach the site of inflammation. Therefore, we investigated the possibility of a more targeted delivery approach, with injection of Treg in or close to the site of inflammation. This approach might require lower Treg numbers compared to systemic infusion and exclude the need for expansion. To test our hypothesis we made use of a humanized mouse model for skin inflammation. The choice for skin as a model to explore local application of Treg was made on the basis that it is easy accessible and supported by the fact that Treg in skin are highly important for tissue repair and reduction of skin inflammation²⁰. We used the so-called huPBL-SCID-huSkin allograft model.

In this model, human skin is transplanted to immune deficient mice and allowed to heal for 3 weeks. Thereafter, allogeneic peripheral blood mononuclear cells (PBMC) are infused by intraperitoneal (IP) injection. In time (2–3 weeks) an immune response mainly consisting of human T cells establishes as demonstrated by the influx of human T cells in the skin, peripheral blood and secondary lymphoid organs^{21–23}. This human-skin allograft model resembles human plaque-type psoriasis at multiple levels, as indicated by erythema and skin thickening, acanthosis, parakeratosis and psoriasis like rete ridges, increased expression of hBD-2, K16 and reduced K10 expression and a strong influx of T cells²¹. This model also reveals similarities with the graft-versus-host-disease (GVHD) of the skin that might occur after stem cell transplantation, including increased expression of Elafin by keratinocytes²¹, which has been shown to be a biomarker of GVHD of the skin^{21,24}.

In a variety of humanized mouse models, including our own, systemic injection of high numbers of Treg, i.e. Treg:PBMC ratio's of 1:5/1:10, was required to inhibit the inflammatory response against islet²⁵, arterial²⁶, and skin^{15,21} allografts. Previously it has been demonstrated that following Treg infusion in a similar humanized skin allograft BALB/c Rag2^{−/−}cγ^{−/−} model that at a Treg:PBMC ratio of 1:10 the immunosuppressive effect of Treg infusion was lost²⁷. Using our humanized mouse allograft SCID/beige model similar observations were made (data not shown).

Here, we demonstrate that low numbers of Treg applied locally can successfully dampen skin inflammation. Where possible, this finding paves the way for the development of protocols that focus on local delivery, without the need for prior *ex vivo* Treg expansion.

Results

Intradermal injection of low dose freshly isolated Treg inhibits skin inflammation. To assess the effectiveness of intradermally applied Treg in the inhibition of human skin inflammation, we first determined the minimal amount of intradermally injected Treg that were needed to inhibit epidermal thickening as part of the inflammatory process in the huPBL-SCID-huSkin allograft model. A range of $2.5\text{--}10 \times 10^4$ high purity FACS sorted human Treg were injected intradermally together with 4×10^7 allogeneic IP injected PBMC. FACS sorted Treg were typically >96% pure CD4⁺CD25^{hi} cells and more than 90% of these cells were FOXP3⁺ (Fig. 1A). IP injection of human allogeneic PBMC alone induced epidermal thickening of the grafted human skin (PBS 126.0 μm (36–163 μm), PBMC 580.0 μm (276–580 μm), $p = 0.0765$), as also described previously²¹. We found that at least $7.5\text{--}10 \times 10^4$ Treg were needed to inhibit this process (thickness: 272 μm (244–301 μm) and 269.5 μm (214–325 μm), respectively (Fig. 1B)).

Based on these results, we selected a dose of 1×10^5 intradermally injected Treg and 4×10^7 IP injected PBMC (a Treg:PBMC ratio of 1:400) to be used for subsequent experiments. Intradermal injection of this low dose of Treg prevented hyperkeratosis (Fig. 2A,E) (PBS 163.0 μm (36–212 μm), PBMC 301.3 μm (142–580 μm), PBMC + Treg 214.0 μm (64–335.8 μm) (PBMC vs PBMC + Treg $p = 0.0395$), and prevented parakeratosis and acantosis, as well as the inflammation induced reduction of K10 expression (Fig. 2B,F) (PBS = 50.9% (24.6–67.2%), PBMC = 4.4% (0–27.3%), PBMC + Treg = 44.2% (5.6–65.2%) (PBMC vs PBMC + Treg $p = 0.002$)). Expression of K16 en hBD2 was analysed by immunofluorescence, and quantified by measuring the median fluorescent expression levels (MFI) in the epidermis (Fig. 2C,D). Low dose Treg injection inhibited the inflammation induced expression (MFI) of K16 (Fig. 2C,G) (PBS = 1883 (1609–2051), PBMC = 5267 (3950–6543) and PBMC + Treg = 4056 (2021–6993), PBS vs PBMC $p = 0.0014$; PBMC vs PBMC + Treg $p = 0.0252$) and hBD2 (Fig. 2D,H) (PBS = 1089 (1049–1153), PBMC = 1364 (1220–2005) and PBMC + Treg = 1221 (1116–1333), PBS vs PBMC $p = 0.0014$, PBMC vs PBMC + Treg $p = 0.0039$).

Skin inflammation in the huPBL-SCID-huSkin allograft model is largely driven by the influx of human T cells into the dermis²¹. Intradermal injection of low dose Treg significantly inhibited the influx of human CD3⁺ T-cells in the dermis (PBS = 282 (117–373) cells/mm², PBMC = 1700 (842–4197) cells/mm² and PBMC + Treg = 784 (142–3202) cells/mm², PBS vs PBMC $p = 0.0014$, PBMC vs PBMC + Treg, $p = 0.0252$) (Fig. 3A,D). We observed that the injection of Treg did not influence the influx of CD8⁺ T cells (Fig. 3B,E), (PBS 0–359.3 cells/mm² (median 0 cells/mm²), PBMC 0–389.5 (median 56.69/mm²), PBMC + Treg 0–437.8 cells/mm² (median 190.6 cells/mm²); hence the observed reduction in CD3⁺ cells is likely due to a reduced influx of CD4⁺ T cells. Although we did not observe a significant increase in the absolute number of human FOXP3⁺ Treg in the human dermis after injection of Treg (Fig. 3C,F) (PBMC 0–154.7 cells/mm², (median 38.6 cells/mm²), PBMC + Treg 0–125.1 cells/mm², (median 72.1 cells/mm²)), a significant increase was found in the ratio of CD3:FOXP3 (Fig. 3G) (PBMC median ratio 49:1, PBMC + Treg median ratio 11:1, $p = 0.0082$). This suggests that intradermal injection of Treg in the mouse skin leads to a relative increase in FOXP3⁺ cells in the human dermis and local inhibition of the inflammatory response.

Having established that intradermal injection of Treg in close proximity to the inflamed skin is effective, we next wondered if this close proximity is actually required to mediate the inhibitory effect of the Treg. Thus we set out to inject Treg at the contralateral (CL) side of the skin graft. Data are presented as the right column of Figs 2 and 3. The data show that also contralateral injection results in reduced epidermal thickening (epithelial thickness 111.2–421.4 μm (median 191 μm) $p = 0.0182$), restoration of the K10/K16 conversion (K10 = 12.5–64.8% (median 13.10), $p = 0.05$ and K16 MFI = 1985–3749 (median 2867) $p = 0.0182$, down regulation of hBD2

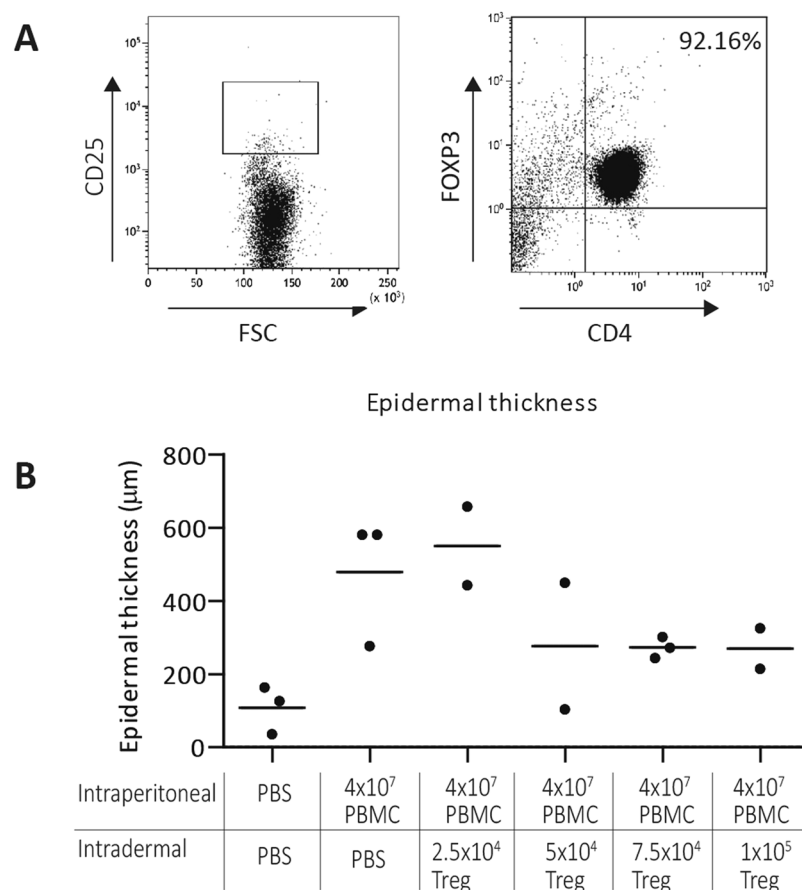


Figure 1. CD4⁺ CD25^{high} gating strategy and dose response curve of freshly isolated non-expanded Treg. **(A)** Gating strategy for sorting CD4⁺ CD25^{high} Treg from isolated CD4⁺ T cells, and flow cytometric analysis of FOXP3 expression after sorting. **(B)** Dose-response curve showing epidermal thickness of human transplanted skin in the huPBL-SCID-huSkin allograft model upon IP PBMC injection without or with intradermal injection of increasing doses of Treg (X-axis). Every dot in the figure represents data from a single mouse.

(MFI = 1098–1142 (median 1120), $p = 0.0182$), and reduced cell influx (CD3 = 185.5–460.6 cells/mm² (median 323.1 cells/mm²), $p = 0.0182$).

Low dose intradermal injection of Treg affects systemic repopulation of human lymphocytes.

To assess whether next to local effects intradermal injection of Treg also exerted systemic effects we analyzed secondary lymphoid organs. After harvesting and processing spleen and draining lymph nodes (LN), the obtained cells were analyzed by flow cytometry. Following intraperitoneal injection of human-PBMC in the skin-transplanted immunodeficient SCIDbeige mice there is clear expansion of the infused T cells that is considered as repopulation, which can be visualized measuring the expression the human leukocyte marker anti-human-CD45 by flow cytometry^{21,28}. IP injection of 4×10^7 PBMC resulted in systemic repopulation of human CD45⁺ lymphocytes in the mouse spleen and LN, which is in line with previous findings^{15,21}. We observed an average of 7.4% human CD45⁺ cells in the LN and 0.63% CD45⁺ cells in the spleen. Intradermal injection of 1×10^5 Treg inhibits human lymphocyte repopulation in LN (2.28%, NS.) and spleen (0.2%, $p = 0.0111$). (Fig. 4A,B). Although the percentages of human CD4⁺ and CD8⁺ T cells within the CD45⁺ population were similar in LN and spleen (Fig. 4C,D), the percentage of CD45⁺CD4⁺FOXP3⁺ T cells were significantly increased in LN and spleen following intradermal Treg injection. (LN 15.6% in PBMC, 29.0% in PBMC + Treg $p = 0.0175$; Spleen 11.7% in PBMC, 29.6% in PBMC + Treg $p = 0.0175$) (Fig. 4E). Taken together, these results show that low dose intradermal Treg injection influences not only the local, but also systemic inflammatory response in the huPBL-SCID-huSkin allograft model.

Discussion

Severe inflammatory skin diseases like severe psoriasis are often treated with biologics, which target the proinflammatory cytokine signaling pathways of TNF α , IL-23 and IL-17. Although these biologics are very successful in the treatment of psoriasis, a substantial group of patients does not respond to this treatment. This urges the quest for novel treatment modalities. Treg-based immune therapy might be a future option. Recently, successful clinical trials with Treg have been conducted in stem cell and solid organ transplantation as well as in (auto) inflammatory diseases such as type-1 diabetes and uveitis^{9,12,29–32}. Also Treg based therapy is considered in the

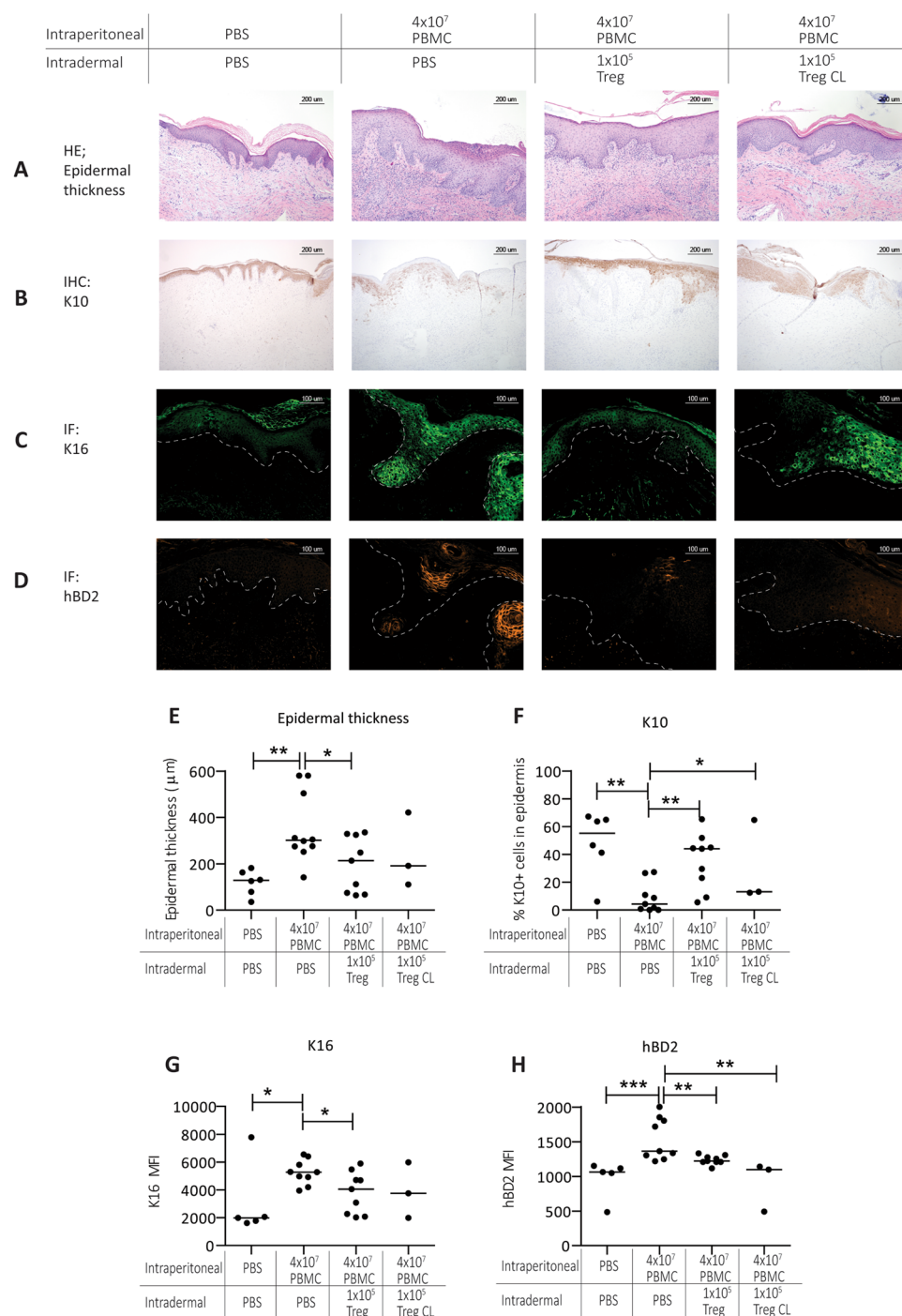


Figure 2. Inhibition of epidermal thickening, sustained K10 expression and absence of K16 and hBD2 up regulation in the epidermis of the human skin after intradermal Treg injection. Representative histology of human skin grafts from SCID beige mice 21 days after IP injection with huPBMC with or without intradermal low dose Treg injection showing: (A) epidermal thickness (HE staining), and the expression of (B). K10 (IHC), (C). K16 and (D). hBD2 (IF). The cell injection conditions are indicated at the top. The most right panel shows the effect of injecting Treg at the contralateral side of the transplanted skin (E–H). Cumulative data showing the median of the epidermal thickness, percentage K10, and median expression levels (MFI) of K16 and hBD2. Every dot in the figure represents a single mouse experiment (n = 3–10). Statistical significance was analyzed by the Mann Whitney U test. *P < 0.05. **P < 0.01.

treatment of refractory Crohn's disease¹¹. An advantage of Treg therapy might be realization of infectious immune suppression, known as a self-perpetuating mechanism of immune suppression. Biologics on the other hand need to be administered life-long.

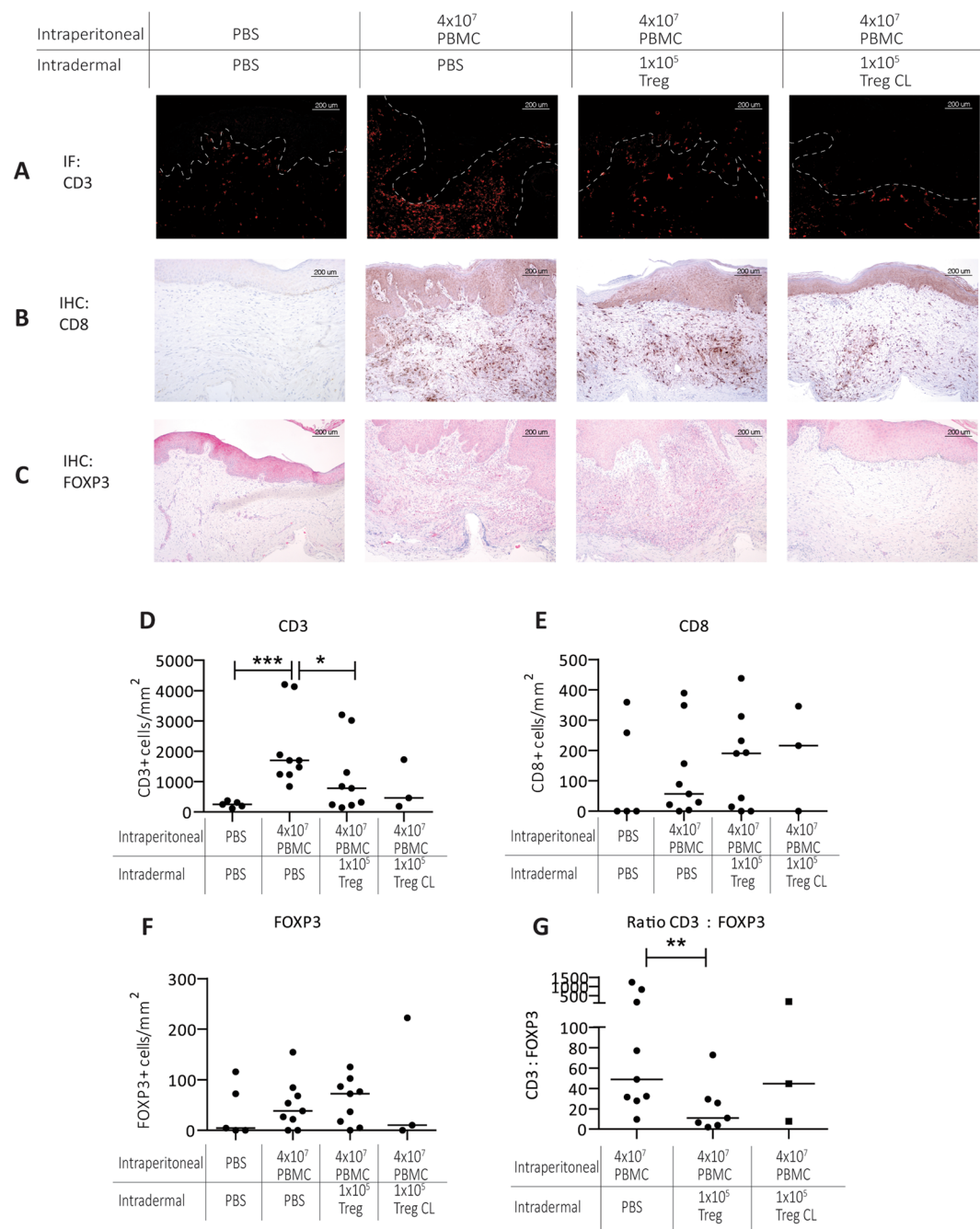


Figure 3. Intradermal Treg injection inhibits the T cell influx and promotes FOXP3+ cells in the human dermis. Representative histology of human skin grafts from SCID beige mice 21 days after IP injection with huPBMC with or without intradermal low dose Treg injection showing (A). CD3, (B). CD8 and (C). FOXP3 cell counts per mm² in the dermis (D–F). Cumulative data figures showing the median of the cells counts. (G) Ratio of CD3:FOXP3 in the dermis. Every dot in the figure represents a single mouse experiment (n = 3–10). Statistical significance was analyzed by the Mann Whitney U test. *P < 0.05. **P < 0.01.

The application of Treg based therapy is studied in clinical transplantation and auto-inflammatory disease^{2,4}, typically using intravenous infusion of large numbers of Treg (e.g. 1–10 million cells/kg in the ONE study³³). To obtain high numbers of Treg these cells have to be expanded *ex vivo* prior to use^{13,15–18}. *Ex vivo* Treg expansion is a critical and laborious step that also introduces the risk of Treg conversion into pro-inflammatory cytokine producing cells¹⁹. We here hypothesized that targeted delivery of Treg at the site of inflammation might require lower numbers of Treg, thereby circumventing large scale *ex vivo* expansion with its drawbacks. In the present study, we demonstrate that intradermal injection of very low numbers of freshly isolated, non-expanded, human Treg can inhibit skin inflammation in the humanized mouse huPBL-SCID-huSkin allograft model.

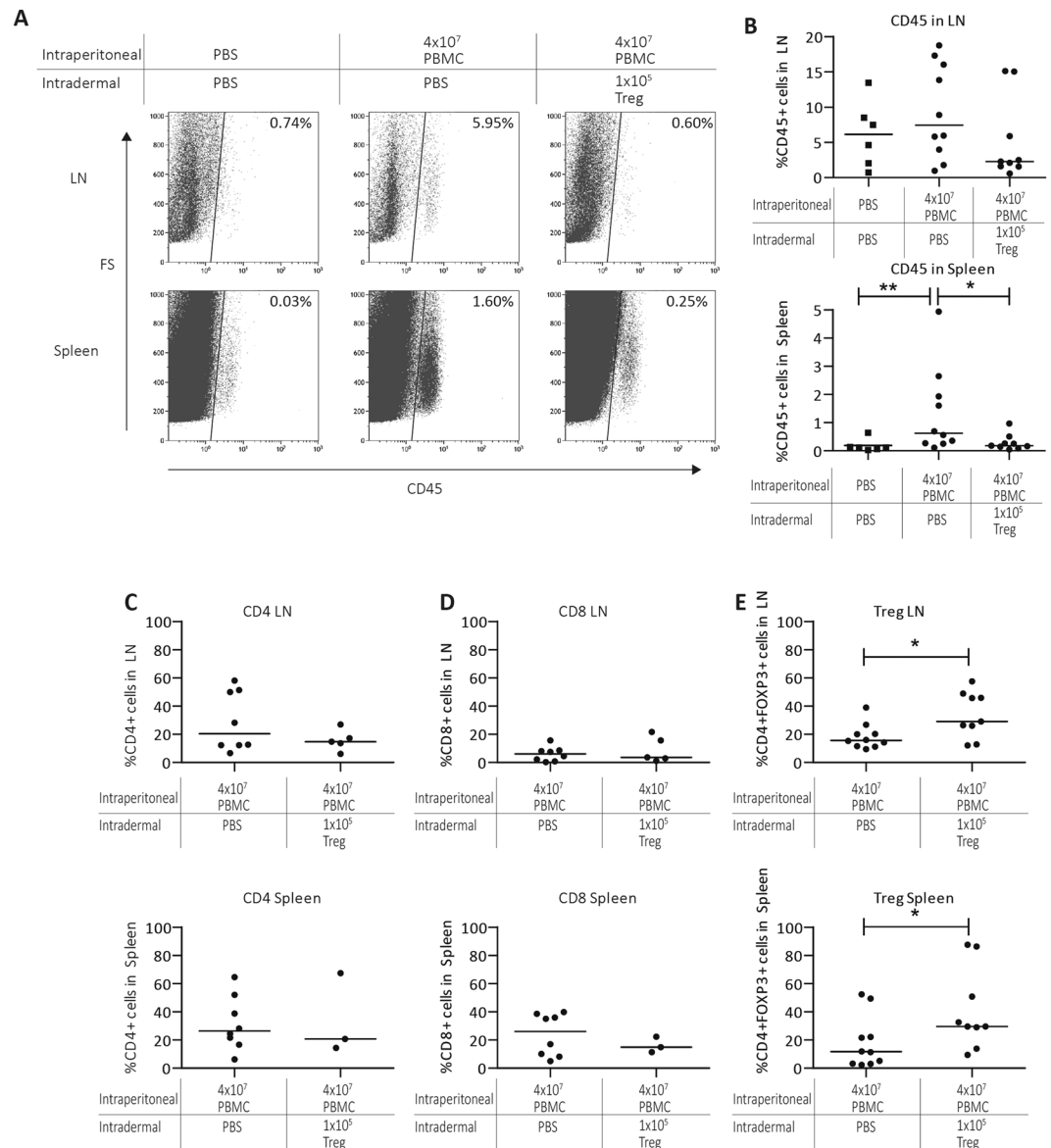


Figure 4. Intradermal Treg injection prevents repopulation of huPBMC and results in a relative increase of CD4+ FOXP3+ cells in the secondary lymphoid organs. **(A)** Representative flow cytometry pictures showing human CD45 expression in single cell suspensions from draining LN and spleen from SCID beige mice 21 days after IP injection with huPBMC with or without intradermal low dose Treg injection. Cumulative data figures showing the median percentages of human **(B)**, CD45+ cells and **(C)**, CD4+, **(D)**, CD8+, **(E)** CD4+ FOXP3+ cells within the CD45+ cells in draining in LN (upper row) and spleen lower row). N = 3–10 Statistical significance was analyzed by the Mann Whitney U test. *P < 0.05.

Systemic administration of Treg, either by intravenous or intra peritoneal injection, may well require high numbers of Treg because the injected cells will be distributed throughout the circulation and tissues and as a consequence a substantial part of the infused cells will be lost³⁴. This appears not to be the case when Treg are injected locally, as we demonstrate here. As for now, we can only speculate why intradermal Treg injection is so efficient. The skin is a complex organ, that next to its strong barrier function, has an important role in the immune defence³⁵ and reveals active trafficking of immune cells such as antigen presenting cells and T cells^{36,37}. The local skin environment facilitates optimal migration to the draining lymphoid organs and control of the immune response. This is supported by skin based vaccination strategies that in humans resulted in highly efficient immunization³⁸. Interesting in this respect are intradermal dendritic cell (DC) vaccination trials that resulted in superior antitumor T-cell induction and faster transit to draining LN^{39–42}. Since intradermal Treg injection in our model led to inhibition of systemic human immune cell reconstitution, it is likely that intradermally injected Treg travel towards the draining LN and regulate the immune response at the level of the secondary lymphoid organs. The notion of a more systemic immune suppressive effect is further strengthened by our observation that injection of Treg at the contralateral side of the animal, and thus far distant from the human transplant, also

inhibited inflammation of the graft. Although local intradermal injection of low Treg numbers seems to impair the systemic immune response, we advise scientist interested in the suppressing systemic inflammation to validate these findings.

Although our current work shows for the first time that small numbers of intradermally injected Treg inhibit inflammation *in vivo*, it appeared technically challenging to demonstrate where and how these little numbers of Treg exerted *in vivo* suppression. In our current work we focused on biodistribution analysis by both fluorescence and radioactive tracking of the injected Treg. CFSE-based cell labeling is possibly of interest for short term-tracking (ie 1–3 days), but appeared not suited to for long-term (3 weeks) biodistribution analysis of intradermal injected Treg (data not shown). Additionally we focused on radioactivity-based biodistribution analysis and survival of the injected Treg by radioactive ¹¹¹Indium labeling of the cells combined with whole body scan SPECT-CT imaging. However, after multiple endeavors of labeling of human Treg with ¹¹¹Indium-oxinate the labeling procedure turned out to be challenging; the labeling efficiency of the isolated Treg was poor and their survival after the labeling was low and unfortunately did not allow for biodistribution and survival analysis. Future studies should focus on optimizing Treg labeling and *in vivo* tracking procedures in order to demonstrate the survival and biodistribution of the intradermally injected cells and to further demonstrate their mechanism of action.

In our model, we have been infusing Treg in the skin with the idea to prevent skin inflammation. The skin is an easily accessible organ, the question is if local delivery of Treg is feasible in case of solid organ transplantation or autoimmune disease such as type-1 diabetes (T1D) or Crohn's disease, which are obviously less accessible. Our data suggests that intradermal Treg infusion promotes Treg migration to the secondary lymphoid organs and controls the immune response there. In fact, in human LNs we have previously demonstrated that Treg are activated and that a substantial number of the Treg is proliferating⁴³. This suggests that secondary lymphoid organs are a physiological platform to organize Treg output. In case of Treg-based therapy in organ transplantation, T1D or Crohn's disease intra nodal injection of Treg in the draining LNs might facilitate local control of the immune response. Intra nodal injection of dendritic cells is already successfully clinically applied in tumor vaccination protocols⁴⁴.

Taken together, targeted intradermal administration of low dose Treg seems to offer a feasible approach for Treg therapy that omits the need for laborious and costly *ex vivo* Treg expansion and reduces the risk of Treg plasticity.

Materials and Methods

Humanized mouse model; huPBL-SCID-huSkin allograft model. The huPBL-SCID-huSkin allograft model used in this study is described in detail by de Oliveira *et al.*²¹. Female B17.B6-Prkdc^{scid}Lysf^{bg}/Crl (SCID beige) mice, 8–12 weeks old (Charles River Breeding Laboratories) were transplanted with human skin from healthy individuals obtained after abdominal plastic surgery at Bauland kliniek (Mill, the Netherlands). After healing of the human skin (21 days), 4×10^7 PBMCs were injected IP in the absence or presence of 2.5×10^4 – 1×10^5 intradermally injected Treg. All animal experimental procedures were in accordance with the international welfare guidelines and approved by the institutional animal ethical committee of the Radboud University in Nijmegen (DEC 2013–023). The use of human skin and peripheral blood were approved and in accordance with the regulations set by the Medical Ethical Committee for human research of the Radboudumc. Human skin and buffy coats (Sanquin Blood Bank, Nijmegen, the Netherlands) were obtained from healthy donors, who gave written consent for scientific use according to the declaration of Helsinki. All experiments were performed in accordance with relevant guidelines and regulations.

Mice were sacrificed 3 weeks after cell injection by orbita extraction followed by cervical dislocation. Terminating the experiment after 3 weeks allows us to study skin inflammation before skin is rejected. In rare cases rejection with GVHD like symptoms, like excessive proliferation of PBMCs in LN and/or spleen, are seen. These mice are excluded from the analysis after ending the experiment with the following exclusion criteria: > 5% CD45+ cells in spleen and/or >20% CD45+ cells in LN as measured with FACS.

Regulatory T cell injection. PBMCs were isolated from buffy coats using ficoll density gradient isolation (Lymphoprep, Nycomed-Pharma AS, Oslo, Norway). To isolate human CD4+ CD25hi Treg, first CD4+ T cells were enriched using the RosetteSep™ (StemCell™ Technologies, Vancouver, Canada) human CD4+ T cell enrichment cocktail according to the manufacturers description, followed by high purity CD4+CD25^{high} cell sorting using a BD FACSARIA cell sorter (BD Biosciences, Erembodegem, Belgium). For this purpose, cells were labeled with CD4-BV510 and CD25-Pe-Cy7(M-A251; BD Biosciences, New Jersey, USA). This typically resulted in >96% pure CD4+CD25^{hi} cells and more than 90% of these cells were FOXP3⁺. Without *ex vivo* expansion, high purity sorted Treg (or PBS, vehicle control) were injected intradermally in the mouse skin at 4 spots closely around the human skin graft, in a total volume of 100 µl PBS.

Histology. Human skin grafts were fixed in neutral buffered 4% formalin (Mallinckrodt Baker Inc, Deventer, the Netherlands) for 4 hours and processed in a Tissue-Tek VIP tissue processor and embedded in paraffin. 6 µm sections of human skin transplants were stained with hematoxylin-eosin (HE) or processed for either immunohistochemical (IHC) or immunofluorescent (IF) staining. Keratinocyte differentiation was analyzed using antibodies against keratin 10 (K10, IHC, RKSE60, Sanbio, Uden, The Netherlands) and keratin 16 (K16, IF, LL025, BioTrend, Koln, Germany). Anti-Human β-defensin 2 (hBD2, IF, Ab9871, Abcam, Cambridge, UK) was used as a marker for the innate skin inflammatory response. For the detection of T cells the following antibodies were used: anti-CD3 (IF, A0452, DAKO, Glostrup, Denmark), anti-CD8 (IHC, 144B, Dako), and anti-FOXP3 (IHC, PCH101, eBioscience, ThermoFisher Scientific, Waltham, USA). For IHC, antibody stainings were visualized using the EnVision + system-HRP (Dako) combined with 3,3',4,4'-diaminobenzidine tetrahydrochloride

(DAB, brown metal enhanced DAB 1856090 ThermoScientific) or using the Labeled Streptavidin Biotin method (Universal LSAB Kit/AP; Dako) combined with Permanent Red (Dako). For IF, nuclei were stained and embedded using DAPI (fluormount-G with DAPI, eBioscience). The secondary antibody for K16 was AF488-conjugated donkey anti-mouse IgG (ThermoFisher); for hBD2 AF546-conjugated donkey anti-goat (ThermoFisher), and for CD3 AF647-conjugated donkey anti-rabbit (ThermoFisher). Sections were photographed using a microscope (AxioImager M2; Zeiss, Sliedrecht, the Netherlands) and a high resolution color camera for bright field microscopy (AxioCam 105 color, Zeiss) and a high resolution b/w camera for multichannel fluorescence microscopy (AxioCam 503 Mono).

Image analysis of histology. Mean epidermal thickness was calculated using AxioVision software version 4.8 (Zeiss) or ZEN blue edition version 2.3 (Zeiss) as epidermal area divided by epidermal surface length. For quantification of K10 positive cells, images were saved at 10x objective magnification. The total epidermal area and K10 positive area were measured using ImageJ in the region of interest (ROI) and displayed as % K10 positive epidermal area. To determine the number of CD8+ and FOXP3+ cells, representative pictures were made at 10 × objective magnification. To quantify the cell counts in the dermis, a representative ROI was drawn from the lowest epidermal papilla till 300 µm dept in the dermis. Cells in this region were counted and expressed as the number of cells per mm². For quantification of K16 and hBD2 positive cells, images were made at 20x objective magnification. The median fluorescent intensity (MFI) in epidermis was determined using ZEN blue (Zeiss). CD3+ cells were counted in the dermis using ZEN blue and expressed as the number of cells per mm².

Flow Cytometry. Spleen and mesenteric lymph nodes (LN) were harvested and cells were obtained by mashing over a 40 µm filter. Single cell suspensions of spleen and LN were phenotypically analyzed using a Navios multi-color flow cytometer (Beckman-Coulter, Mijdrecht, the Netherlands). Human leukocytes were identified using an antibody directed against the common human leukocyte marker CD45 (anti-human-CD45-KO (J33, Beckman-Coulter). For cell-surface staining of human CD4 and CD8 T cells, the following antibodies were used: anti-CD4-PC5.5 (13B8.2, Beckman Coulter), and anti-CD8-APC-AF700 (B9.11, Beckman-Coulter). For intracellular staining with anti-FOXP3-e450 (PCH101, eBioscience), cells were fixed and permeabilized by fix-perm treatment (eBioscience) according to manufacturers instruction. Data were analyzed using Kaluza software version 1.5a (Beckman-Coulter) and gates were set based on single staining and FMOs (Supplemental Fig. 1)

Data and Statistics. Statistical analysis was performed using GraphPad Prism software version 5.03 (Graphpad Software Inc., San Diego, US). The median of the data points is displayed unless mentioned otherwise. Groups were compared using Mann Whitney U test. Differences with a p-value of <0.05 were considered significant and are indicated with an asterisk (*). p < 0.01 is indicated as**.

References

1. Sakaguchi, S., Miyara, M., Costantino, C. M. & Hafler, D. A. FOXP3+ regulatory T cells in the human immune system. *Nature reviews. Immunology* **10**, 490–500, <https://doi.org/10.1038/nri2785> (2010).
2. Bluestone, J. A., Trotta, E. & Xu, D. The therapeutic potential of regulatory T cells for the treatment of autoimmune disease. *Expert opinion on therapeutic targets* **19**, 1091–1103, <https://doi.org/10.1517/14728222.2015.1037282> (2015).
3. Cabello-Kindelan, C., Mackey, S. & Bayer, A. L. Adoptive T Regulatory Cell Therapy for Tolerance Induction. *Current transplantation reports* **2**, 191–201, <https://doi.org/10.1007/s40472-015-0058-5> (2015).
4. Issa, F., Chandrasekharan, D. & Wood, K. J. Regulatory T cells as modulators of chronic allograft dysfunction. *Current opinion in immunology* **23**, 648–654, <https://doi.org/10.1016/j.coi.2011.06.005> (2011).
5. Issa, F. & Wood, K. J. CD4+ regulatory T cells in solid organ transplantation. *Current opinion in organ transplantation* **15**, 757–764, <https://doi.org/10.1097/MOT.0b013e32834017ae> (2010).
6. Brunstein, C. G. *et al.* Umbilical cord blood-derived T regulatory cells to prevent GVHD: kinetics, toxicity profile, and clinical effect. *Blood* **127**, 1044–1051, <https://doi.org/10.1182/blood-2015-06-653667> (2016).
7. Martelli, M. F. *et al.* HLA-haploidentical transplantation with regulatory and conventional T-cell adoptive immunotherapy prevents acute leukemia relapse. *Blood* **124**, 638–644, <https://doi.org/10.1182/blood-2014-03-564401> (2014).
8. Todo, S. *et al.* A pilot study of operational tolerance with a regulatory T-cell-based cell therapy in living donor liver transplantation. *Hepatology (Baltimore, Md.)* **64**, 632–643, <https://doi.org/10.1002/hep.28459> (2016).
9. Bluestone, J. A. *et al.* Type 1 diabetes immunotherapy using polyclonal regulatory T cells. *Science translational medicine* **7**, 315ra189, <https://doi.org/10.1126/scitranslmed.aad4134> (2015).
10. Marek-Trzonkowska, N. *et al.* Factors affecting long-term efficacy of T regulatory cell-based therapy in type 1 diabetes. *Journal of translational medicine* **14**, 332, <https://doi.org/10.1186/s12967-016-1090-7> (2016).
11. Desreumaux, P. *et al.* Safety and efficacy of antigen-specific regulatory T-cell therapy for patients with refractory Crohn's disease. *Gastroenterology* **143**(1207–1217), e1201–1202, <https://doi.org/10.1053/j.gastro.2012.07.116> (2012).
12. Gregoire, S. *et al.* Treatment of Uveitis by *In Situ* Administration of *Ex Vivo*-Activated Polyclonal Regulatory T Cells. *Journal of immunology (Baltimore, Md.: 1950)* **196**, 2109–2118, <https://doi.org/10.4049/jimmunol.1501723> (2016).
13. Canavan, J. B. *et al.* Developing *in vitro* expanded CD45RA+ regulatory T cells as an adoptive cell therapy for Crohn's disease. *Gut* **65**, 584–594, <https://doi.org/10.1136/gutjnl-2014-306919> (2016).
14. Bovenschen, H. J. *et al.* Foxp3+ regulatory T cells of psoriasis patients easily differentiate into IL-17A-producing cells and are found in lesional skin. *The Journal of investigative dermatology* **131**, 1853–1860, <https://doi.org/10.1038/jid.2011.139> (2011).
15. He, X. *et al.* A TNFR2-Agonist Facilitates High Purity Expansion of Human Low Purity Treg Cells. *PloS one* **11**, e0156311, <https://doi.org/10.1371/journal.pone.0156311> (2016).
16. Landwehr-Kenzel, S. *et al.* Novel GMP-compatible protocol employing an allogeneic B cell bank for clonal expansion of allospecific natural regulatory T cells. *American journal of transplantation: official journal of the American Society of Transplantation and the American Society of Transplant Surgeons* **14**, 594–606, <https://doi.org/10.1111/ajt.12629> (2014).
17. Putnam, A. L. *et al.* Clinical grade manufacturing of human alloantigen-reactive regulatory T cells for use in transplantation. *American journal of transplantation: official journal of the American Society of Transplantation and the American Society of Transplant Surgeons* **13**, 3010–3020, <https://doi.org/10.1111/ajt.12433> (2013).
18. Scotta, C. *et al.* Differential effects of rapamycin and retinoic acid on expansion, stability and suppressive qualities of human CD4(+) CD25(+)FOXP3(+) T regulatory cell subpopulations. *Haematologica* **98**, 1291–1299, <https://doi.org/10.3324/haematol.2012.074088> (2013).

19. Koenen, H. J. *et al.* Human CD25highFoxp3pos regulatory T cells differentiate into IL-17-producing cells. *Blood* **112**, 2340–2352, <https://doi.org/10.1182/blood-2008-01-133967> (2008).
20. Ali, N. & Rosenblum, M. D. Regulatory T cells in Skin. *Immunology*, <https://doi.org/10.1111/imm.12791> (2017).
21. de Oliveira, V. L. *et al.* Humanized mouse model of skin inflammation is characterized by disturbed keratinocyte differentiation and influx of IL-17A producing T cells. *PLoS one* **7**, e45509, <https://doi.org/10.1371/journal.pone.0045509> (2012).
22. Murray, A. G. *et al.* Human T-cell-mediated destruction of allogeneic dermal microvessels in a severe combined immunodeficient mouse. *Proceedings of the National Academy of Sciences of the United States of America* **91**, 9146–9150 (1994).
23. Murray, A. G. *et al.* Dermal microvascular injury in the human peripheral blood lymphocyte reconstituted-severe combined immunodeficient (HuPBL-SCID) mouse/skin allograft model is T cell mediated and inhibited by a combination of cyclosporine and rapamycin. *The American journal of pathology* **153**, 627–638, [https://doi.org/10.1016/s0002-9440\(10\)65604-0](https://doi.org/10.1016/s0002-9440(10)65604-0) (1998).
24. Paczesny, S. *et al.* Elafin is a biomarker of graft-versus-host disease of the skin. *Science translational medicine* **2**, 13ra12, <https://doi.org/10.1126/scitranslmed.3000406> (2010).
25. Wu, D. C. *et al.* Ex vivo expanded human regulatory T cells can prolong survival of a human islet allograft in a humanized mouse model. *Transplantation* **96**, 707–716, <https://doi.org/10.1097/TP.0b013e31829fa271> (2013).
26. Nadig, S. N. *et al.* In vivo prevention of transplant arteriosclerosis by ex vivo-expanded human regulatory T cells. *Nature medicine* **16**, 809–813, <https://doi.org/10.1038/nm.2154> (2010).
27. Issa, F., Hester, J., Milward, K. & Wood, K. J. Homing of regulatory T cells to human skin is important for the prevention of alloimmune-mediated pathology in an in vivo cellular therapy model. *PLoS one* **7**, e53331, <https://doi.org/10.1371/journal.pone.0053331> (2012).
28. Issa, F. *et al.* Ex vivo-expanded human regulatory T cells prevent the rejection of skin allografts in a humanized mouse model. *Transplantation* **90**, 1321–1327, <https://doi.org/10.1097/TP.0b013e3181ff8772> (2010).
29. Marek-Trzonkowska, N., Mysliwiec, M., Siebert, J. & Trzonkowski, P. Clinical application of regulatory T cells in type 1 diabetes. *Pediatric diabetes* **14**, 322–332, <https://doi.org/10.1111/pedi.12029> (2013).
30. Trzonkowski, P. *et al.* First-in-man clinical results of the treatment of patients with graft versus host disease with human ex vivo expanded CD4+ CD25+ CD127– T regulatory cells. *Clinical immunology (Orlando, Fla.)* **133**, 22–26, <https://doi.org/10.1016/j.clim.2009.06.001> (2009).
31. Brunstein, C. G. *et al.* Infusion of ex vivo expanded T regulatory cells in adults transplanted with umbilical cord blood: safety profile and detection kinetics. *Blood* **117**, 1061–1070, <https://doi.org/10.1182/blood-2010-07-293795> (2011).
32. Lombardi, G. *et al.* Cell therapy to promote transplantation tolerance: a winning strategy? *Immunotherapy* **3**, 28–31, <https://doi.org/10.2217/imt.11.42> (2011).
33. McMurchy, A. N., Bushell, A., Levings, M. K. & Wood, K. J. Moving to tolerance: clinical application of T regulatory cells. *Seminars in immunology* **23**, 304–313, <https://doi.org/10.1016/j.smim.2011.04.001> (2011).
34. Sharif-Paghaie, E. *et al.* In vivo SPECT reporter gene imaging of regulatory T cells. *PLoS one* **6**, e25857, <https://doi.org/10.1371/journal.pone.0025857> (2011).
35. Richmond, J. M. & Harris, J. E. Immunology and skin in health and disease. *Cold Spring Harbor perspectives in medicine* **4**, a015339, <https://doi.org/10.1101/cshperspect.a015339> (2014).
36. Tomura, M. *et al.* Activated regulatory T cells are the major T cell type emigrating from the skin during a cutaneous immune response in mice. *The Journal of clinical investigation* **120**, 883–893, <https://doi.org/10.1172/jci40926> (2010).
37. Egawa, G. & Kabashima, K. Skin as a peripheral lymphoid organ: revisiting the concept of skin-associated lymphoid tissues. *The Journal of investigative dermatology* **131**, 2178–2185, <https://doi.org/10.1038/jid.2011.198> (2011).
38. Chen, D., Bowersock, T., Weeratna, R. & Yeoh, T. Current opportunities and challenges in intradermal vaccination. *Therapeutic delivery* **6**, 1101–1108, <https://doi.org/10.4155/tde.15.65> (2015).
39. Pizzurro, G. A. & Barrio, M. M. Dendritic cell-based vaccine efficacy: aiming for hot spots. *Frontiers in immunology* **6**, 91, <https://doi.org/10.3389/fimmu.2015.00091> (2015).
40. Harris, R. C. *et al.* The vaccine-site microenvironment induced by injection of incomplete Freund's adjuvant, with or without melanoma peptides. *Journal of immunotherapy (Hagerstown, Md.: 1997)* **35**, 78–88, <https://doi.org/10.1097/CJI.0b013e31823731a4> (2012).
41. Lesterhuis, W. J. *et al.* Route of administration modulates the induction of dendritic cell vaccine-induced antigen-specific T cells in advanced melanoma patients. *Clinical cancer research: an official journal of the American Association for Cancer Research* **17**, 5725–5735, <https://doi.org/10.1158/1078-0432.ccr-11-1261> (2011).
42. Kersey, T. W., Van Eyk, J., Lannin, D. R., Chua, A. N. & Tafra, L. Comparison of intradermal and subcutaneous injections in lymphatic mapping. *The Journal of surgical research* **96**, 255–259, <https://doi.org/10.1006/jsre.2000.6075> (2001).
43. Peters, J. H. *et al.* Human secondary lymphoid organs typically contain polyclonally-activated proliferating regulatory T cells. *Blood* **122**, 2213–2223, <https://doi.org/10.1182/blood-2013-03-489443> (2013).
44. Bol, K. F. *et al.* Intranasal vaccination with mRNA-optimized dendritic cells in metastatic melanoma patients. *Oncoimmunology* **4**, e1019197, <https://doi.org/10.1080/2162402x.2015.1019197> (2015).

Acknowledgements

We would like to thank Rob Woestenink, Gaby Derksen, Bram van Cranenbroek, Esther van Rijssen and Kelly Warmink, as well as all animal care takers and technicians at the EBD of the Central Animal Facility of the Radboudumc for technical support. Also, we thank Prof. O Boerman and Janneke Molkenboer for their help with the ¹¹¹Indium-labeling studies. Also, we thank members of the EU COST BM1305 consortium AFACCT for meaningful discussion.

Author Contributions

S.L. designed and performed the experiments, coordinated the study, analyzed the data and wrote the manuscript. V.d.O. performed experiment and analyzed data. E.F. participated in data collection and analyzed the data. S.B. participated in data collection. P.v.E., I.J. and H.K. co-supervised the study, developed concept and design of the study and wrote the paper. All authors reviewed the manuscript and agreed with its content.

Additional Information

Supplementary information accompanies this paper at <https://doi.org/10.1038/s41598-018-28346-5>.

Competing Interests: The authors declare no competing interests.

Publisher's note: Springer Nature remains neutral with regard to jurisdictional claims in published maps and institutional affiliations.



Open Access This article is licensed under a Creative Commons Attribution 4.0 International License, which permits use, sharing, adaptation, distribution and reproduction in any medium or format, as long as you give appropriate credit to the original author(s) and the source, provide a link to the Creative Commons license, and indicate if changes were made. The images or other third party material in this article are included in the article's Creative Commons license, unless indicated otherwise in a credit line to the material. If material is not included in the article's Creative Commons license and your intended use is not permitted by statutory regulation or exceeds the permitted use, you will need to obtain permission directly from the copyright holder. To view a copy of this license, visit <http://creativecommons.org/licenses/by/4.0/>.

© The Author(s) 2018